Ideal tensile and shear strength of β-C_3N_4 from first-principles calculations

Yi Zhang,[1,2] Hong Sun,[1,2] and Changfeng Chen[2]
[1]*Department of Physics, Shanghai Jiao Tong University, Shanghai 200030, China*
[2]*Department of Physics and High Pressure Science and Engineering Center, University of Nevada, Las Vegas, Nevada 89154, USA*
(Received 10 April 2007; revised manuscript received 6 July 2007; published 3 October 2007)

Covalent solid β-C_3N_4 has received considerable attention in the last two decades since it was predicted to be a superhard material based on its high bulk modulus that is comparable to that of diamond. Here, we report first-principles calculations that examine its deformation modes and its ideal tensile and shear strength at large strains. The calculated results show that the ideal tensile and shear strength of β-C_3N_4 are both much lower than those of diamond; more significant, they are even below those of cubic boron nitride (c-BN) despite that c-BN is elastically more compliant near equilibrium. This illustrates the disparity between the mechanical properties of β-C_3N_4 at equilibrium and at large strains. The different bonding structures of β-C_3N_4 from those of diamond and c-BN introduce more complex structural deformation modes. We discuss the microscopic mechanism of the structural deformation in β-C_3N_4 under different strains and, in particular, examine the role of the angular deformation of the C-N bonds and its effects on the overall stress-strain relations. The results provide insights for understanding its mechanical properties at large strains at the atomic level. The knowledge may also prove useful for the design of new strong covalent solids.

DOI: 10.1103/PhysRevB.76.144101 PACS number(s): 62.20.Fe, 81.40.Jj

I. INTRODUCTION

The search for new superhard materials is an important field of research in material science and technology. Inspired by the successful synthesis of diamond and cubic boron nitride (c-BN) in laboratory, studies of other strong covalent solids have been actively pursued over the years. Considerable efforts have been devoted to finding new materials that have excellent mechanical performance and enhanced chemical stability. Based on a semiempirical formula, Cohen suggested that β-C_3N_4 may be a potential superhard material that can compete with diamond in strength and hardness.[1–3] Later, other C_3N_4 polymorphs (α-, pseudocubic and cubic) were also proposed.[4–8] They all have large calculated bulk moduli that are used as a strong indicator for their potential high strength and hardness. Carbon nitrides also attract great interests for their other remarkable physical properties such as wide band gap,[3,8,9] negative Poisson ratio,[10] and high thermal conductivity.[11] In the past decade, many groups reported successful synthesis of carbon nitrides, especially the β-C_3N_4. A variety of deposition techniques were employed, including chemical vapor deposition,[12] sputtering,[13,14] and ion implantation.[15] By using pulsed laser deposition, Niu *et al.* prepared C-N thin film in which the β-C_3N_4 crystallites were identified.[16] Most recently, Yin *et al.* reported successful growth of single crystal β-C_3N_4 nanorods.[17] Lv *et al.* prepared a mixture of crystalline powder that mainly includes $\alpha-C_3N_4$ and β-C_3N_4.[18] On the theoretical side, a lot of effort has been devoted to exploring the properties of carbon nitrides using first-principles calculations.[19–24]

Despite their questionable stability and insufficient experimental evidence of pure crystalline phases, C_3N_4 polymorphs have been actively pursued for their potential extreme hardness and strength that are highly desirable in many applications. This is based on their large calculated elastic parameters. However, the elastic parameters, such as bulk and shear moduli at equilibrium, may not give an accurate account for the strength or hardness at large strains introduced by the deformation processes involved in applications or testing measurements. Large structural deformation can produce significant changes in bonding characters, which usually result in a nonlinear stress-strain relation and sometimes unexpected bond softening and breaking. As a result, simple extrapolations from the equilibrium properties may not be reliable.[25–28] A more stringent test for material strength at large strains is provided by the calculation of the ideal strength, i.e., the stress at which a perfect crystal lattice becomes mechanically unstable, that sets an upper bound for material strength. It should be noted that the measured value of hardness of a material depends on a number of factors, including the type of indenter, the measurement procedure, and the magnitude and rate of the applied force (pressure), among others.[29] On the other hand, the yield and ideal strength are well defined physical quantities that can be calculated accurately. Recent experiments have reported successful measurements of the yield[30] and ideal[31] strength of materials. Moreover, the ideal strength study also can give insights into the structural deformation process at the atomic level, which leads to a better understanding of the relation between chemical bonding and macroscopic properties of covalent solids under strain.[32,33] Discussions on material hardness based on ideal strength results should make distinction of these two types of quantities, although a positive correlation between them does exist and is useful for understanding the mechanical properties and the underlying mechanisms.[29]

Recent ideal strength calculations on the hypothetical pseudocubic C_3N_4 revealed a significant strain induced C-N bond weakening during structural deformation.[34] This result contradicts with the previous understanding about the correlation between local bonding characters and the strength and hardness of covalent solids, namely, that the short C-N bonds should lead to high strength at large strains. The physical explanation for the weak C-N bonding in pseudocubic C_3N_4 is that the sp^3 electron state from the N atom forming the C-N bond is high in energy that tends to break the sp^3 C-N

bond under the external stress and form the new C-N bond with sp^2 electron states from N and C atoms.[34] In the study of strong crystalline carbon nitrides, the α- and β-C_3N_4 phases are the primary focus since these are the phases identified in all reported experiments. They have similar sp^3 and sp^2 hybridized bonding structures and are predicted to have large hardness and strength. However, no ideal strength studies for these two phases have been reported because of their relatively large unit cells that make calculations of the stress-strain relations more costly. These calculations are nevertheless desirable since these are the experimentally synthesized phases and, consequently, the relation between the elastic moduli near equilibrium and the ideal strength at large strains would have more practical significance and relevance. Furthermore, the bonding environment in their structures is more complex and quite different from those of the cubic and pseudocubic structures. The C-N bonds in the α- and β-C_3N_4 phases are formed between the stable sp^3 electron state from the C atom and sp^2 electron state from the N atom, which are expected to be stronger than the C-N bonds in pseudocubic C_3N_4. It would be interesting to investigate the effect of the difference in local bonding structure on the ideal strength of these strong covalent solids.

II. METHOD OF CALCULATION

In this paper, we report on a systematic study of the ideal strength of β-C_3N_4 under tensile and shear deformation using first-principles calculations. Its local bonding structures are nearly identical to those in $\alpha-C_3N_4$ whose unit cell is twice as large as that of β-C_3N_4. The total energy is computed as a function of strain using the local-density-approximation pseudopotential scheme with a plane-wave basis set.[35–37] The norm-conserving Troullier-Martins pseudopotentials[38] were used with cutoff radii of 1.3 a.u. for N and C. The exchange correction functional of Ceperley and Alder[36] as parametrized by Perdew and Zunger[39] was used. The total energy of the structure was minimized by relaxing the structural parameters using a quasi-Newton method.[40] The total energy and stress calculations used a $4\times4\times8$ Monkhorst-Pack[41] k-point grid and a 100 Ry energy cutoff. The error in stresses caused by the energy cutoff and k-point grid is less than 0.1 GPa based on convergence tests.

The β-C_3N_4 unit cell, shown in Fig. 1, contains 14 atoms and has a $P6_3/m$ symmetry. Each N atom is coordinated with three C atoms forming sp^2 bonding and each C site is connected to four N tetrahedrally. As pointed out in Ref. 5, a subtle difference exists in bonding characters between two typical N sites in β-C_3N_4, which are denoted as N_A and N_B to represent the N sites attached to or being included in the 12 atom hexagonal ring, respectively. The fully relaxed results show that the length of C-N bond (1.454 Å) with its N site belonging to the N_A type is 0.7% larger than that (1.443 Å) with N belonging to the N_B type. The detailed equilibrium structural data are listed in Table I. The calculated lattice constants a_0 and c_0 agree well with the previous results. They are slightly larger than Hashimoto and Kohyama's results[24] and smaller than Teter and Hemley's[6] that were obtained under the $P3$ symmetry. The calculated lattice parameters are close to those measured in the recently synthesized crystalline β-C_3N_4 (a=6.43 Å, c=2.43 Å).[18] We have calculated elastic constants and compared with previously reported data, as shown in Table II. In these calculations, a series of small positive and negative strains is applied to the equilibrium structure and all the atoms in the unit cell are fully relaxed. The five independent elastic constants are obtained by fitting the energy-strain curves. For the hexagonal β-C_3N_4, the criteria of mechanical stability are C_{11}, $C_{11}-C_{12}$, C_{44}, and $(C_{11}+C_{12})C_{33}-2C_{13}^2$ all being positive. Our present results satisfy these conditions.

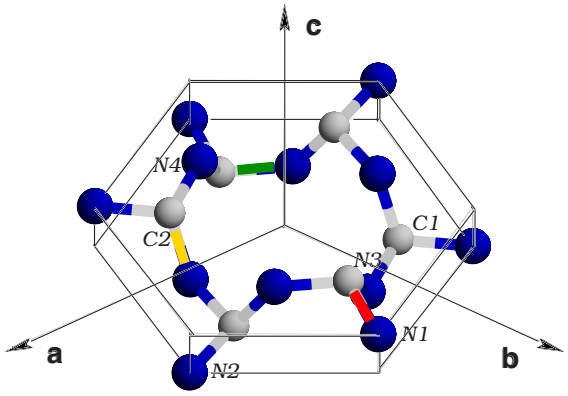

FIG. 1. (Color online) The relaxed $P6_3/m$ β-C_3N_4 structure with its unit cell depicted by the solid line frame. The independent atomic positions that determine the structure of β-C_3N_4 are denoted, where the N1 and N2 sites belong to the N_A type and the N3 and N4 sites to the N_B type (see the text for details on the distinction of these sites).

For the calculation of the ideal strength along the deformation paths in various directions, we employed a method described in detail previously.[42,43] The lattice vectors were incrementally deformed in the direction of the applied strains. At each step, the atomic basis and all the atoms inside the unit cell were simultaneously relaxed until all the components of the Hellmann-Feynman stress tensor orthogonal to the applied strains were less than 0.1 GPa. To identify the weakest tensile direction, we calculated the tensile stresses along various crystallographic directions for β-C_3N_4. The critical shear stress was then calculated by applying shear deformations in the easy-slip plane perpendicular to the weakest tensile direction. Different from the strong covalent solids with cubic symmetry such as diamond and c-BN, β-C_3N_4 is low in structural anisotropy due to its cage-like bonding configuration (see Fig. 1). We examined the stress responses along the directions of high symmetry since the deformations allowed by symmetry can lower the energy and lead to energetically favorable relaxation pathways for structural transformation or failure. We also examined tensile deformations along the directions of the bond alignment in various directions. This is because along these directions, the bonds are stretched most effectively under strain, leading to relatively quick bond weakening and structural failure.[32]

TABLE I. The calculated structural parameters of β-C_3N_4. The coordinates of each atom are given relative to the lattice vectors. To compare our results with those previously reported, the atomic sites N4, C1, and C2 are translated from their original positions by $\vec{a}+\vec{b}$, $\vec{a}$, and $\vec{b}$, respectively (marked by *).

		Present work	Teter and Hemley[a]	Hashimoto and Kohyama[b]
		$P6_3/m$	$P3$	$P6_3/m$
a(Å)		6.388	6.4017	6.377
c(Å)		2.398	2.4041	2.393
c/a		0.3754	0.3755	0.3752
$N1$	x	1/3	1/3	1/3
	y	2/3	2/3	2/3
	z	3/4	3/4	3/4
$N2$	x	2/3	2/3	2/3
	y	1/3	1/3	1/3
	z	1/4	1/4	1/4
$N3$	x	0.0329	0.0331	0.0328
	y	0.3303	0.3309	0.3302
	z	0.2500	0.2502	0.2500
$N4^*$	x	0.9671	0.9669	0.9672
	y	0.6697	0.6705	0.6698
	z	0.7500	0.7498	0.7500
$C1^*$	x	0.7728	0.7732	0.7726
	y	0.1782	0.1784	0.1781
	z	0.2500	0.2499	0.2500
$C2^*$	x	0.2272	0.2271	0.2274
	y	0.8218	0.8216	0.8219
	z	0.7500	0.7501	0.7500

[a]Reference 6.
[b]Reference 24.

III. RESULTS AND DISCUSSION

We first calculated the elastic moduli of β-C_3N_4 and, for comparison, diamond and c-BN. The results are listed in Table III. The bulk moduli were obtained by fitting the Birch-Murnaghan equation of state, and the shear moduli were obtained by taking the average of the tetragonal $[(C_{11}-C_{12})/2]$ and rhombohedral $[C_{44}]$ shear moduli. Also listed are the predictions of the hardness and available experimental results on these materials. β-C_3N_4 has relatively large bulk and shear moduli that are 95% and 56% of those for diamond, with a predicted Vickers hardness of 85.7 GPa. This hardness value is remarkably high: it is only 12% lower than that of diamond and 33% higher than that of c-BN. These data seem to support the conclusion that β-C_3N_4 is indeed a superhard solid, although it does not exceed diamond in hardness as originally proposed. However, the predicted hardness data are based on the structural and electronic properties of the equilibrium structure.[45] Despite the good agreement between the measured and calculated data for diamond and c-BN, which is consistent with the ideal strength calculations,[32] it is still necessary to determine the ideal strength of β-C_3N_4 to examine the structural behavior at large strains. To this end, we calculated the stress-strain relations under tensile deformation in the $\langle 120\rangle$, $\langle 100\rangle$, and $\langle 001\rangle$ crystallographic directions and obtained the peak stresses at 62.2, 70.6, and 83.0 GPa, respectively. These results identify the $\langle 120\rangle$ direction as the weakest tensile direction, which indicates that under tensile loadings, β-C_3N_4 would likely cleavage in the $\langle 120\rangle$ direction. However, the differences in the tensile strength among these directions are not as large as those of diamond and c-BN.[32] This leaves some degree of ambiguity in the natural cleavage preference of β-C_3N_4. It is noted (see Table IV) that despite its large elastic moduli, the ideal tensile strength of β-C_3N_4 is much lower than that of diamond and even below that of c-BN that has a bulk modulus 9% smaller than that of β-C_3N_4. The situation is similar for the ideal shear strength. These results indicate that β-C_3N_4 may not be as strong or hard as sug-

TABLE II. Five calculated elastic constants (Calc.) for β-C_3N_4 in comparison with previous calculation (Liu and Wentzcovitch). All the data are in GPa units.

	C_{11}	C_{33}	C_{44}	C_{12}	C_{13}
Calc.	896	1110	293	281	121
Liu and Wentzcovitch[a]	834	1120	305	279	138

[a]Reference 4.

TABLE III. The calculated (Calc.) bulk modulus (B_0) and shear modulus (G_0) of β-C_3N_4 (all in GPa), in comparison with previous calculations (Prev.) and experiments (Expt.). Results of Vickers hardness (H_0) are presented as a reference. No measured values are available for β-C_3N_4.

	β-C_3N_4		Diamond		c-BN	
	Calc.	Prev.	Calc.	Expt.	Calc.	Expt.
B_0	437	437[a]	459	443[b]	393	368[b]
G_0	300	320[a]	534	525.5[b]	391.5	397.5[b]
H_0		85.7[c]	97.3[c]	96±5[d]	64.5[c]	63±5[d]

[a]Reference 7.
[b]Reference 44.
[c]Reference 45.
[d]Reference 46.

TABLE IV. The calculated ideal tensile and shear stresses of β-C_3N_4, in comparison with those of diamond and c-BN.

	Tensile $\langle 120\rangle$	Shear (120)[100]
β-C_3N_4 (GPa)	62.2	60.5
	Tensile $\langle 111\rangle$	Shear $(111)\langle 11\bar{2}\rangle$
Diamond (GPa)	92.9	96.3
c-BN (GPa)	65.6	70.5

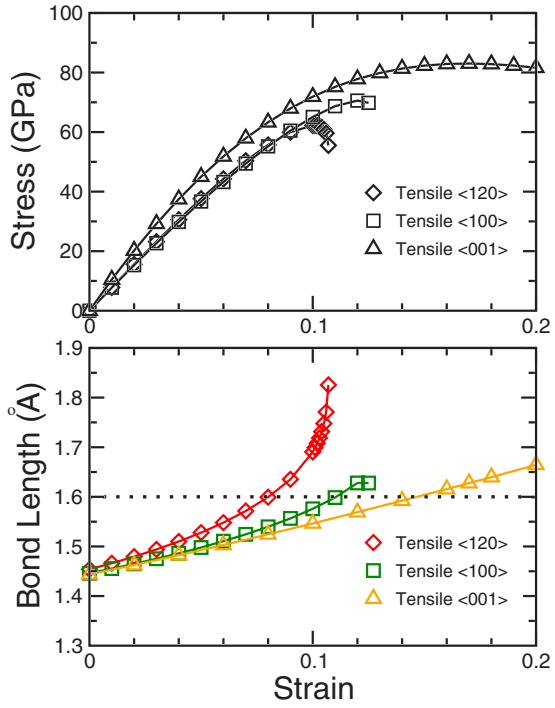

FIG. 2. (Color online) The calculated stress and length of the most stretched bonds as functions of strain along the ⟨120⟩, ⟨100⟩, and ⟨001⟩ tensile directions.

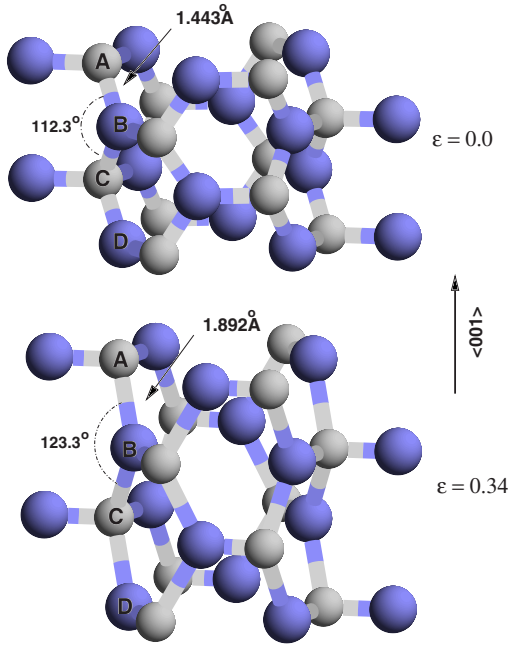

FIG. 3. (Color online) The snapshots of β-C_3N_4 at equilibrium (ϵ=0.0) and at a very large strain of ϵ=0.34 corresponding to the critical point for bond breaking under the ⟨001⟩ tension. Several atoms are labeled to show their movements in the tensile deformation process.

gested by its elastic properties at equilibrium.[2,6,7,45]

We now turn to a detailed analysis of the atomistic structural deformation modes in β-C_3N_4 to examine the microscopic mechanism of its reduced (from the expectation based on the elastic moduli at equilibrium) ideal strength and the fracture behavior under the tensile and shear loading conditions. Figure 2 shows the calculated stress- and bond-length-strain relations of β-C_3N_4 under tensile strains along three principal symmetry directions. At small strains, the tensile stresses in all three directions exhibit a steep and almost linear rise in the stress-strain curves, indicating large elastic constants at or near the equilibrium structure. This is in agreement with previous results mentioned above. The variations of stress and bond length under ⟨120⟩ and ⟨100⟩ tensile strains are nearly identical because of the low structural anisotropy. Furthermore, under these tensile strains, the material becomes unstable right after passing the maximum stress point. Meanwhile, under the ⟨001⟩ tensile strain, it undergoes a long deformation process while maintaining a plateau of high stress response. This is because in the former case (especially in the ⟨120⟩ direction), the tensile strain directly stretches the C-N bonds that are aligned in the same direction, causing direct bond stretch and breaking. Under the ⟨001⟩ tension, there are no bonds aligned in the direction of the applied stress; the zigzag C-N chain structure (see Fig. 3) provides an additional channel for structural deformation through the variation of the angular degree of freedom that allows a further and gradual structural deformation. It extends the deformation range before the structural failure. Figure 3 shows two structural snapshots, one at equilibrium (ϵ=0) and another at a large strain of ϵ=0.34 corresponding to the critical point for bond breaking (which is beyond the range shown in Fig. 2, but the stress is still quite large at this point) under the ⟨001⟩ tension. In this process, the corresponding bond angle changes from 112.3° to 123.3° and the length of C-N bonds in the chain is elongated from 1.443 to 1.892 Å along the *ABCD* chain. The angular deformation mode allows the bonds to remain relatively short and strong over a large deformation range in this tensile deformation process and is responsible for the significant extension of the range of strain with large stress. In contrast, under the ⟨120⟩ and ⟨100⟩ tensile strains, the bond angles change only slightly while the bond length increases at a much higher rate, especially under the ⟨120⟩ stress (see Fig. 2). For the C-N bonds that stretch the most in the tensile directions (Fig. 2), they show an almost linear response to increasing strain until the bond length reaches a critical point. In β-C_3N_4, this point is estimated to be 1.6 Å and the tensile strains corresponding to the peak stresses are 0.08, 0.11, and 0.14 in ⟨120⟩, ⟨100⟩, and ⟨001⟩ directions, respectively.

We now examine the stress-strain relation and the deformation modes of β-C_3N_4 under shear strains. In Fig. 4, we plot the calculated shear stress as a function of the applied shear strains in the easy-slip (120)[100] direction. It is noticed that a nearly linear relation extends all the way to the breaking point at ϵ=0.266. Right before the breaking point, the unit cell distorts significantly, which leads to a distribution of the applied strain over all the bonds through both the direct bond-length stretching and bond-angle bending in the unit cell (see the bottom part of Fig. 4). The largest bond-length increase (to 1.510 Å) of β-C_3N_4 under the (120) [100] shear strain up to the bond breaking point is only 4.7% of its initial length (1.443 Å). This is similar to what occurs under the ⟨001⟩ tension but is very different from the situation in

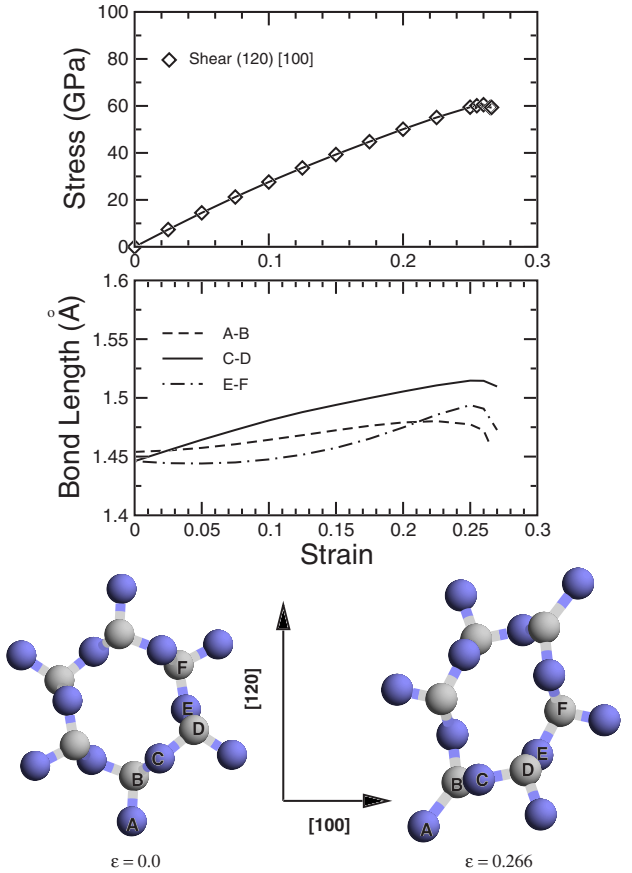

FIG. 4. (Color online) The calculated stress-strain relation (top panel) and bond-length variation for a few most stretched bonds (middle panel) along the path of the (120) [100] shear strain for β-C_3N_4. The local bonding structures at equilibrium (ϵ=0) and at the critical strain ϵ=0.266 corresponding to the peak (ideal) shear stress are shown at the bottom. Several atoms are labeled to show their movements under the shear deformation.

the cubic structures of diamond and *c*-BN where the bonds can be sheared up to 1.715 and 1.705 Å, respectively, which are 11.9% and 9.6% larger than their initial lengths at equilibrium.[32] Here, the global distribution of the load on a large number of C-N bonds and the combined stretch and twisting (angular) deformation modes during the shear deformation significantly reduce the range of the bond-length variation, which results in the nearly linear behavior in the stress-strain relation, as shown in Fig. 4. In contrast, the anisotropic configuration of the bonds in zinc-blende structures would result in a smaller number of bonds being predominantly stretched in the shear deformation processes. It can easily lead to the change of their local bonding characters and a display of the nonlinear stress-strain relation before reaching the critical breaking point.[32]

For covalent solids with the zinc-blende structure, like diamond and *c*-BN, a transition from cubic to graphitic phase induced by the applied $\langle 111\rangle$ tensile and (111) $\langle 11\bar{2}\rangle$ shear strains is expected at large strains.[32] However, our calculations did not yield such structural transformation for β-C_3N_4. In fact, no stable structures were found beyond the peak stress point under all applied strains considered despite

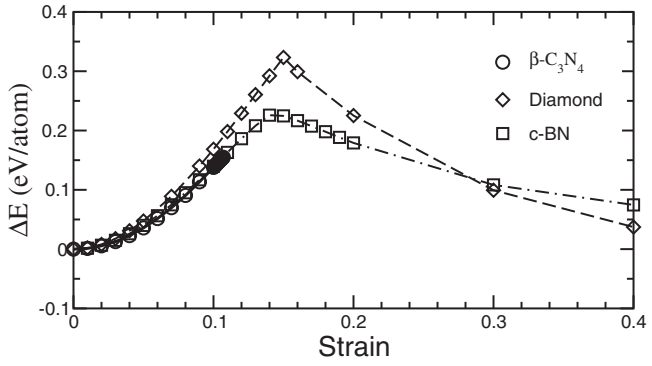

FIG. 5. The calculated energy variation versus strain of β-C_3N_4, diamond, and *c*-BN along their weakest tensile deformation directions ($\langle 120\rangle$, $\langle 111\rangle$, and $\langle 111\rangle$, respectively).

extensive structural relaxation efforts. This is likely due to the limited size of the unit cell used in the calculations that is inadequate to describe possible phase transitions to structures with much larger unit cells. The calculated deformation energy barrier of β-C_3N_4 in the [120] tensile direction is only 0.155 eV/at., that is, only about 50% and 69% of those of diamond and *c*-BN, respectively (Fig. 5). This result shows that β-C_3N_4 is not very stable and can transform into other (yet to be characterized) structures by overcoming the low energy barrier.

IV. SUMMARY

In summary, we have performed first-principles calculations to study the atomistic deformation modes and the ideal strength of β-C_3N_4 under tensile and shear strains. The calculated results indicate that the $\langle 120\rangle$ direction is the easy cleavage direction under tensile stresses. However, the differences in the peak stresses along other directions are not as large as those in diamond and *c*-BN, thus leaving some degree of ambiguity in the cleavage fracture patterns for β-C_3N_4 under different loading conditions that may have various resolved stresses along the principal tensile directions. The ideal shear strength is obtained under the (120) [100] shear deformation path. The obtained ideal tensile and shear strength of β-C_3N_4 are lower than those of diamond and *c*-BN, although its bulk modulus is comparable to that of diamond and larger than that of *c*-BN. These results illustrate the disparity between mechanical properties at or near equilibrium and at large strains and point to the need for a careful analysis of structural deformation at large strains. Similar to the sp^3 C-N bonds in pseudocubic C_3N_4,[34] the obtained low ideal strength of β-C_3N_4 indicates that the C-N bonds formed by the sp^3 electron of C and sp^2 electron of N are also weak at large strains, which may be a general character of these C-N bonds. The deformation of the cagelike structure of β-C_3N_4 shows modes different from those of zinc-blende structures. In particular, the angular deformation modes play an important role in yielding a long range of large stress response under the $\langle 001\rangle$ tension. It is also noted

that β-C_3N_4 exhibits an almost linear stress response to the applied strains in various deformation modes. This can be attributed to the low anisotropy of the structure and the relatively small stretch of bond length before bond breaking. Its low potential energy barrier may explain why it is difficult to synthesize large size β-C_3N_4 crystals in experiment. This knowledge provides insights for understanding the mechanical properties of β-C_3N_4 and may also prove useful in the design of new strong covalent solids.

ACKNOWLEDGMENTS

This work was supported by the Department of Energy under Cooperative Agreement No. DE-FC52-06NA26274 at UNLV. H.S. and Y.Z. were also supported by the National Natural Science Foundation of China Grants Nos. 10574089 and 50532020, Chinese National Minister of Education Program for Innovative Research Team in University, and the High Performance Computing Center at Shanghai Jiao Tong University.

[1] M. L. Cohen, Phys. Rev. B **32**, 7988 (1985).
[2] A. Y. Liu and M. L. Cohen, Science **245**, 841 (1989).
[3] A. Y. Liu and M. L. Cohen, Phys. Rev. B **41**, 10727 (1990).
[4] A. Y. Liu and R. M. Wentzcovitch, Phys. Rev. B **50**, 10362 (1994).
[5] A. Reyes-Serrato, D. H. Galvan, and I. L. Garzon, Phys. Rev. B **52**, 6293 (1995).
[6] D. M. Teter and R. J. Hemley, Science **271**, 53 (1996).
[7] D. M. Teter, MRS Bull. **23**, 22 (1998).
[8] J. L. Corkill and M. L. Cohen, Phys. Rev. B **48**, 17622 (1993).
[9] H. Yao and W. Y. Ching, Phys. Rev. B **50**, 11231 (1994).
[10] Y. Guo and W. A. Goddard III, Chem. Phys. Lett. **237**, 72 (1995).
[11] M. L. Cohen, Solid State Commun. **92**, 45 (1994).
[12] T. Y. Yen and C. P. Chou, Appl. Phys. Lett. **67**, 2801 (1995).
[13] H. Sjostrom, S. Stafstrom, M. Boman, and J. E. Sundgren, Phys. Rev. Lett. **75**, 1336 (1995).
[14] K. M. Yu, M. L. Cohen, E. E. Haller, W. L. Hansen, A. Y. Liu, and I. C. Wu, Phys. Rev. B **49**, 5034 (1994).
[15] S. P. Withrow, J. M. Williams, S. Prawer, and D. Barbara, J. Appl. Phys. **78**, 3060 (1995).
[16] C. Niu, Y. Z. Lu, and C. M. Lieber, Science **261**, 334 (1993).
[17] L. W. Yin, Y. Bando, M. S. Li, Y. X. Liu, and Y. X. Qi, Adv. Mater. (Weinheim, Ger.) **15**, 1840 (2003).
[18] Q. Lv, C. Cao, C. Li, J. Zhang, H. Zhu, X. Kong, and X. Duan, J. Mater. Chem. **13**, 1241 (2003).
[19] Y. G. Yoon, B. G. Pfrommer, F. Mauri, and S. G. Louie, Phys. Rev. Lett. **80**, 3388 (1998).
[20] S. D. Mo, L. Ouyang, W. Y. Ching, I. Tanaka, Y. Koyama, and R. Riedel, Phys. Rev. Lett. **83**, 5046 (1999).
[21] G. M. Rignanese, J. C. Charlier, and X. Gonze, Phys. Rev. B **66**, 205416 (2002).
[22] Z. Y. Liu, J. He, J. Yang, X. Guo, H. Sun, H. T. Wang, E. Wu, and Y. Tian, Phys. Rev. B **73**, 172101 (2006).
[23] J. M. Hu, W. D. Cheng, S. P. Huang, D. S. Wu, and Z. Xie, Appl. Phys. Lett. **89**, 261117 (2006).
[24] T. Hashimoto and M. Kohyama, Phys. Rev. B **64**, 012103 (2001).
[25] S. Ogata, J. Li, and S. Yip, Science **298**, 807 (2002).
[26] S. Ogata, J. Li, N. Hirosaki, Y. Shibutani, and S. Yip, Phys. Rev. B **70**, 104104 (2004).
[27] Y. Zhang, H. Sun, and C. F. Chen, Phys. Rev. Lett. **93**, 195504 (2004); **94**, 145505 (2005).
[28] Z. Pan, H. Sun, and C. F. Chen, Phys. Rev. Lett. **98**, 135505 (2007).
[29] V. V. Brazhkin, A. G. Lyapin, and R. J. Hemley, Philos. Mag. A **82**, 231 (2002).
[30] M. I. Eremets, I. A. Trojan, P. Gwaze, J. Huth, R. Boehler, and V. D. Blank, Appl. Phys. Lett. **87**, 141902 (2005).
[31] T. Li, J. W. Morris, Jr., N. Nagasako, S. Kuramoto, and D. C. Chrzan, Phys. Rev. Lett. **98**, 105503 (2007).
[32] Y. Zhang, H. Sun, and C. F. Chen, Phys. Rev. B **73**, 144115 (2006).
[33] Z. Pan, H. Sun, and C. F. Chen, Phys. Rev. B **73**, 214111 (2006).
[34] Y. Zhang, H. Sun, and C. F. Chen, Phys. Rev. B **73**, 064109 (2006).
[35] J. Ihm, A. Zunger, and M. L. Cohen, J. Phys. C **12**, 4409 (1979).
[36] D. M. Ceperley and B. J. Alder, Phys. Rev. Lett. **45**, 566 (1980).
[37] M. L. Cohen, Phys. Scr., T **T1**, 5 (1982).
[38] N. Troullier and J. L. Martins, Phys. Rev. B **43**, 1993 (1991).
[39] J. P. Perdew and A. Zunger, Phys. Rev. B **23**, 5048 (1981).
[40] B. G. Pfrommer, M. Cote, S. G. Louie, and M. L. Cohen, J. Comput. Phys. **131**, 233 (1997).
[41] H. J. Monkhorst and J. D. Pack, Phys. Rev. B **13**, 5188 (1976).
[42] D. Roundy, C. R. Krenn, M. L. Cohen, and J. W. Morris, Jr., Philos. Mag. A **81**, 1725 (2001).
[43] D. Roundy, C. R. Krenn, M. L. Cohen, and J. W. Morris, Jr., Phys. Rev. Lett. **82**, 2713 (1999).
[44] H. Sun, S. H. Jhi, D. Roundy, M. L. Cohen, and S. G. Louie, Phys. Rev. B **64**, 094108 (2001).
[45] J. L. He, L. C. Guo, X. J. Guo, R. P. Liu, and Y. J. Tian, Appl. Phys. Lett. **88**, 101906 (2006).
[46] R. A. Andrievski, Int. J. Refract. Met. Hard Mater. **19**, 447 (2001).